The T-SCAN™ Technology: Electrical Impedance as a Diagnostic Tool for Breast Cancer Detection

by

Michel Assenheimer, Orah Laver-Moskovitz, Dov Malonek, David Manor, Udi Nahaliel, Ron Nitzan, and Abraham Saad

TransScan Medical, Ltd.*, P.O.Box 786, 10550 Migdal Ha'Emek, Israel

Short Title: Breast Cancer Detection by Electrical Impedance

PACS: 87, 87.19Nn, 87.19Xx, 84.37.+q

Keywords: Electrical Impedance, Breast Cancer, Tissue Differentiation

* Correspondence should be addressed to: ronn@transscan.co.il. Further information can also be found on http://www.transscan.co.il.

Abstract

In this paper we present the T-SCAN™ technology and its use as a diagnostic tool for breast cancer detection. We show, using theoretical models with simplified geometries, that displaying planar two-dimensional maps of the currents detected at the breast's surface relate to the electric field distribution within the breast. This distribution is a manifestation of the bulk spatial inhomogeneities in the complex dielectric constant that represent the various tissue types. These differences may be used to discriminate between various pathological states. We, furthermore, illustrate a useful classifier, based on admittance data measured up to 2 kHz, and we argue that low frequency impedance measurements can be used successfully in breast cancer diagnosis.

1. Introduction

Breast cancer is the leading cause of death in western women aged 35-54. It is expected to reach 1 in 7 women by the year 2000 (American Cancer Society, 1997). Survival rates are highest when it is detected early and still confined to the breast. TransScan TS2000 is a new, noninvasive and radiation-free imaging device for breast examination based on mapping the local electrical impedance properties of breast tissue (Piperno et al., 1990). TransScan's T-Scan™ technology[1] maps non-invasively, in real-time, the local distribution of tissue electrical impedance at various frequencies. The TS2000 systems, in combination with mammography, ultrasound, or clinical breast examination (CBE) have the potential to make a clinically significant and cost-effective methodology for the detection of early stage breast cancer. Previous studies, using a prototype device "Mammoscan" (Piperno et al., 1990), have indicated the potential of the method for early detection of breast cancer.

The basic idea that lies behind the T-Scan™ technology is in the notion that tissues differ in their dielectric parameters. Large differences between neoplastic and normal tissue have been reported by in-vitro measurements on freshly excised breast tissue by Surowiec et al., (1988) and Jossinet (1996, 1998). Measurements taken *in-vivo* from women undergoing surgical excisional biopsy show clear differences in the dielectric properties of cancerous breast tissue and benign tissue (Morimoto et al., 1990). Lately, Brown et al. (2000) presented a study in which current flow measurement can accurately help in the diagnosis of cervical neoplasia in patients that had positive smear tests. These studies describe the physiological basis for the idea that tissue differentiation may plausibly be based on measurements of the dielectric properties.

[1] US Patent 09/150224

In this paper we present the TS2000 device that utilizes variations in electrical properties of tissue for breast cancer diagnosis. The TS2000 system, (TransScan Medical, Ltd. Migdal Haemek, Israel), measures surface currents on the breast, using them for tissue differentiation within the breast. Currently, the system operates in the low frequency range. Here we argue that even though at low frequencies skin impedance is indeed quite large (Rosell et al., 1988), it does not prevent us from performing tissue differentiation within the breast. We demonstrate how to process measured data in order to avoid the skin impedance.

In Section 2, TransScan's measurement technique and analysis methodology is described. Section 3 presents a theoretical model that describes a measurement setup similar to the T-Scan™; a tumor within the breast is represented as a spherical disturbance within otherwise uniform medium in an electric field. In Section 4 modifications to the model are presented, restricting the geometry of the electric field to realistic breast dimensions. In section 5 we introduce a new method of data analysis, which takes into account the masking effect of the skin.

2. The T-SCAN™ technology

In a T-SCAN™ examination, an alternating electric field is applied between the patient's arm and breast. A voltage source is connected to a hand-held electrode, in the form of a stainless steel cylinder. The measuring probe, which contains a multitude of electrodes arranged on a rectangular grid, is placed on the breast and each of its elements is held at virtual ground. The evoked electric current is measured at each of its sensor elements. The TS2000 system is provided with three different probes, having different indications for use (TS2000 User Manual). Our small probe has an eight by eight pad array with a total footprint of 32 by 32 mm. The large probe consists of sixteen by sixteen pad elements with a footprint of about 72 by 72 mm. TransScan's newest probe has the same footprint as our small probe, but with sixteen by sixteen pad elements. The total area occupied by the sensor elements is

optimized for generation of homogenous electric field under the probe. At each of the pads the current is measured using a trans-impedance measurement technique; while the evoked current under a particular pad is measured, all other pads are kept at ground potential. Typically, amplitudes of 1-2.5 volts are applied between the hand held electrode and the breast electrodes with frequencies spanning 100 Hz – 100 kHz. Diagnostics is based on the spectral behavior of the currents, namely the amplitude, the in-phase and the out-of-phase components of the measured currents at the various frequencies. These components are related to the conductance, $\sigma(\omega)$, and dielectric constant, $\varepsilon(\omega)$, respectively. In figure 1 a typical breast exam, performed with the TS2000 system, is shown. The trans-impedance measurement principle is shown in figure 2. When using any one of our probes, signals from the trans-impedance amplifiers are converted to digital signals by customized electronics and transferred to a Pentium PC for further processing. Fast filtering algorithms are utilized for calculating the amplitude and phase of each pad's measured signal. The transmitted source signal is also sampled and serves as a reference signal. These signals coupled with the system's transfer function, are utilized to compute the admittance at each of the pad sensors. Conductance and capacitance related maps are calculated from the measured data and presented to the clinician on the PC monitor. These real-time maps provide guidance for the physician while manipulating the probe prior to and during the measurements. The frame rate for 64-sensor probe is approximately 17 frames per second. The performance of the system was evaluated using multitude of passive components that were selected to represent physiological values. Accuracy of 5% was obtained for capacitance values in the range of 20 pF – 1nF and conductance values in the range of 1-20 μS. The system's signal-to-noise ratios reached nearly 70 dB at low frequencies (100 Hz) and 40dB at high frequencies (up to 100 kHz). Preliminary measurements at frequencies as high as 500KHz have been successfully obtained.

In addition to the probe's sensing circuitry additional safety directed circuitry is included in the system. This over-current sensing circuitry, which is implemented by hardware, provides additional safety mechanism of the system to avoid the possible delivery of high current to the patient.

3. The dipole model – infinite geometry

A globally healthy breast can be considered as a homogenous medium, consisting mostly of fatty tissue, characterized by its complex dielectric properties, $\sigma_1 + i\omega\varepsilon_1$. Consider a small spherical disturbance, such as a cancerous tumor, within the otherwise homogenous breast, whose complex dielectric properties are given by $\sigma_2 + i\omega\varepsilon_2$. Typically, tumors have higher conductance than the surrounding healthy tissue (Surowiec et al., 1988). The evoked electric current travels from the patient's hand to her arm, reaches the highly conducting pectoralis muscle, which may, therefore, be considered as an iso-potential plane, while the probe induces an iso-potential plane as it is held at ground potential. Thus, when the probe is placed on the breast of a patient, lying in a supine position, a roughly parallel electrical configuration is created. In this setup, the lesion (which is assumed to be highly conductive compared to its surrounding tissue) within the breast will distort this presumably homogenous field

The electric field distribution in the medium can be obtained by solving Laplace equation $\nabla\Phi = 0$ with boundary conditions on the sphere (see for example "Classical Electrodynamics" by J.D. Jackson, 2nd Edition, pp150-152). A schematic view of equi-potential lines is given in figure 3. As illustrated in the figure, the pattern of the field lines is identical to the field of a dipole located at the center of the lesion. Hence the term "the dipole model"

The normal field is given by:

$$E_z = E_o + \frac{3kz^2}{(x^2+y^2+z^2)^{5/2}} - \frac{k}{(x^2+y^2+z^2)^{3/2}}$$

$$k = \frac{\varepsilon - 1}{\varepsilon + 2}\rho^3 \qquad \varepsilon = \frac{\sigma_2 + j\omega\varepsilon_2}{\sigma_1 + j\omega\varepsilon_1}$$

or,

$$E_z = E_0\left[1 + \frac{k\left(2z^2 - R^2\right)}{\left(R^2+z^2\right)^{5/2}}\right]$$

with, $R^2 = x^2 + y^2$, $k = \frac{\varepsilon - 1}{\varepsilon + 2}\rho^3$, $\varepsilon = \frac{\sigma_2 + i\omega\varepsilon_2}{\sigma_1 + i\omega\varepsilon_1}$.

Here, ρ is the radius of the disturbance. In principle, it is possible to extract the *depth, size, conductance, and dielectric constant* of the disturbance with respect to the homogenous background. At each sensor element the current is given by Ohm's law, J = σE. The complex relative current distribution is given by:

$$\frac{J_z(R)}{J_0} = \left[1 + \frac{k\left(2z^2 - R^2\right)}{\left(R^2+z^2\right)^{5/2}}\right].$$

Based on the above equation, the depth of the lesion, z_0, can be estimated by performing multiple measurements and solving for *z*. Once z_0 has been obtained, *k* can be retrieved by measuring above the perturbation, i.e. $R = 0$. This yields,

$$\frac{J_z(R_0)}{J_0} = 1 + \frac{2k}{z_0^3}.$$

Since the ε variation, between about 2 and infinity, (ε-1)/(ε+2) which is the multiplier of ρ^3 varies between about 0.25 and 1. Therefore, ρ varies by mare 30% as ε changes between 2 and infinity.

A number of limitations apply: first and foremost, the biological tissue, even the healthy one, is not homogenous, and not even isotropic, in its complex dielectric properties; furthermore, tumors are not exactly spherical, and so forth; second, the applied field is influenced by the finite probe size, even though the guard ring (at zero potential) that surrounds the sensing area, minimizes these edge effects.

4. The dipole model – finite depth geometry

With the dipole model in an infinite medium, the amplitude of the peak current reaches maximum when the disturbance is just below the surface. In this case, the current density amplitude, just above the disturbance, can be as much as 3 times higher than the un-disturbed surroundings. However, when the surrounding medium has finite depth (e.g. a finite distance between the isopotential pectoralis muscle and the probe), this result is no longer valid; in the limiting case of a conducting sphere with a diameter equal to the spacing between conducting plates, the peak current density will be equal to the ratio between the applied voltage and the impedance of the highly conducting sphere. On the other hand, the surrounding current density will be equal to the ratio between the applied voltage and the impedance of the surrounding tissue. Thus, the ratio between the peak current density and the surrounding is equal to the impedance ratio between the tissues (tumor vs. normal) and exceeds the value of 3.

We solved the problem numerically for various geometrical configurations. The simulations were used for studying the effect of varying the distance between the plates and the depth of the sphere below the surface.

In figure 4, the results obtained for simulating both models are presented. At the left side results for finite distance between the plates are shown while at the right side the results for dipole model with infinite geometry are presented. In these simulations we used the radius of

the sphere (ρ) as the basic measurement unit. The relative dielectric constant (i.e. dielectric constant of the conductive sphere relative to that of the surrounding medium) was set to be 50. It is clear from the results, that in the finite depth model, a sphere that is near the measuring plate yields a disturbance image, which is much larger in amplitude and much narrower in its spatial extent than in the infinite geometry model.

Furthermore, the dependence of the amplitude on the depth of the finding is much weaker than the z^{-3} behavior for the dipole model in the infinite geometry, as shown in figure 5.

Figure 5 illustrates the dependence of the relative peak current density ($\Delta J(R)$) on the relative distance between plates and the depth of the sphere is shown. The horizontal axis is the depth of the sphere in units of the sphere's diameter. The top most graph (1) describes the amplitude of the peak current density above background when the distance between plates was 3 times the diameter of the sphere. The other graphs (2-5) show simulation results for an increasing distance between plates: 3.5, 4, 4.5 and 5 times the diameter of the sphere. When the sphere is near the surface the relative peak current density ($\Delta J(R)$) is very high and it decreases as the depth increases. However, when the sphere is located closer to the bottom plate, the relative peak current density starts to rise due to increased current density in the sphere.

This finite depth model describes more adequately the anatomical setup when the T-SCAN™ is used for measurements taken on the breast. Pressing the probe on the breast by the physician during the measurement decreases the distance between the measuring probe and the pectoralis muscle and thus an increase in the relative peak current density is expected.

5. The three-element model

According to Singh et al. (1979), the discrimination between cancerous and benign tissues is best performed below 200Hz. However, at low frequencies the skin impedance

masks the relevant variations of the underlying tissues. The skin can be modeled by a three-element circuit consisting of a conductor G_p in parallel with a capacitor C_p, in series with a second conductor G_s [3]. A similar model applies to the underlying tissues (Rosell et al, 1988; Jossinet 1996,1998). The numerical values for the skin were derived from Rosell et al, (1988) and were the following: $G_p \sim 0.3$ μS, $C_p \sim 1.5$ nF, and $G_s \sim 10$ μS, for area of 0.1 cm^2, while for the underlying tissue, these values were G_p, $G_s > 10$ μS, and $C_p < 0.1$ nF. At low frequencies, the Ohmic current of the tissues is much larger than the corresponding displacement current. Therefore, the parallel tissue capacitor may be neglected, in agreement with the well-known theory of the α-processes (Barber and Brown, 1984). This implies that only the Ohmic current needs to be considered, leaving the tissue to be modeled by a simple series resistor. Thus, we have reduced the problem of skin plus tissue to a three-element model, whose elements we term G_p, C_p, and $R_s = 1/G_s$. Here, G_p and C_p refer to the skin, while G_s defines the tissue. The issue is to extract G_s without the obscuring effect of G_p.

To that purpose, we define the critical frequency as the frequency at which the imaginary part of the admittance Y reaches its maximum. This is obtained by setting $\partial_\omega \mathrm{Im}(Y) = 0$, where the imaginary part of the three-element circuit is given by:

$$\mathrm{Im}(Y) = \frac{\omega C_p}{(1 + R_s G_p)^2 + (\omega C_p R_s)^2} \approx \frac{\omega C_p}{1 + (\omega C_p R_s)^2}$$

resulting in,

$$\omega_c = \frac{G_s}{C_p}$$

It is important to note that ω_c only depends on G_s, and does not suffer from the masking of G_p of the skin. The critical frequency can be evaluated from the phase of measured admittance,

$$\varphi = \tan^{-1}\frac{G}{\omega C} = \tan^{-1}\frac{\omega}{\omega_c}.$$

Here, G and C simply mean the real and imaginary parts of the detected signal. Thus ω_c is given by,

$$\frac{d}{d\omega}\tan\varphi = \frac{1}{\omega_c}.$$

6. Conclusion

In this paper we presented the basic technological aspects of the T-SCAN™. We developed a model that describes the electrical field surrounding a lesion in otherwise homogeneous surroundings. The infinite medium model was extended to take into account finite depths as well as effects of the highly resistive skin. In addition, a three-element model was introduced in attempt to evaluate the admittance characterizing the underlying tissue, omitting the masking effects of the skin.

References

American Cancer Society 1997 Surveillance Research, http://www.cancer.org/statistics

Barber D C and Brown B H 1984 Applied Potential Tomography, *J. Phys. E: Sci. Instrum.* 17, 723

Brown B H Tidy J A Boston K Blackett A D Smallwood R H and Sharp F 2000 Relation between tissue structure and imposed electrical current flow in cervical neoplasia, Lancet, 355, 892-895

Jossinet J 1996 Variability of impedivity in normal and pathological breast tissue, *Med. Biol. Eng. Comput.* 34, 346-350

Jossinet J 1998 The impedivity of freshly excised human breast tissue, *Physiol. Meas.* 19, 61-75

Morimoto T Kinouchi Y Iritani T Kimura S Konishi Y Mitsuyama N Komaki K and Monden Y 1990 Measurement of the electrical bio-impedance of breast tumors, *Eur. Surg. Res.* 22, 86-92

Piperno G Frei E H and Moshitzky M 1990 Breast cancer screening by impedance measurements, Frontiers Med. Biol. Engng., 2, 111-117

Rosell J Colominas J Riu P Pallas P and Webster J G 1988 Skin impedance from 1 Hz to 1 MHz*, IEEE Trans. Biomed. Eng.* 35, 649

Singh B Smith C W and Hughes R 1979 In vivo dielectric spectrometer, *Med. Biol. Eng. Comput.* 17, 45

Surowiec A J Stuchly S S 1988 Dielectric Properties of Breast Carcinoma and the Surrounding Tissues, *IEEE Trans. Biomed. Eng.* 35, 257

TransScan Medical, Ltd., TS2000 User Manual (2000)

Vecchio, T J 1966 Predictive Value of a Single Diagnostic Test in Unselected Populations, N. Engl. J. Med. 274 (21) 1171-1173

Figure captions

Figure 1. A typical breast examination performed with the TS2000 system.

Figure 2. Electronic scheme of the single pad measurement procedure.

Figure 3. Field line distribution outside the lesion. The lesion is located at the center of an otherwise homogenous medium, with thickness of 4.4 lesion diameters. The bottom plate is held at 2.5V while the top plate is held at zero potential. Note the resemblance of the resulting field to the field of a dipole.

Figure 4. Simulation results depicting current density distribution under finite geometry considerations (left) compared with infinite geometry (right). Note the different scales. The finite geometry model is constructed with two metal plates and finite distance between them while the infinite geometry model is constructed with two plates whose inter-distance is very large.

Figure 5. Simulation results depicting the relative peak current density above the disturbance. The X-axis is the depth bellow the sensor array, in lesion diameter units; Y-axis is the relative current density (disturbance / background). The various curves show simulation results for 5 different inter-plate distances. Each curve depicts the peak amplitude vs. lesion depth. Curves 1-5 correspond to inter-plate distances of 3.5, 4, 4.5, 5 and 6 lesion diameters, respectively.

Figure 1

Figure 2.

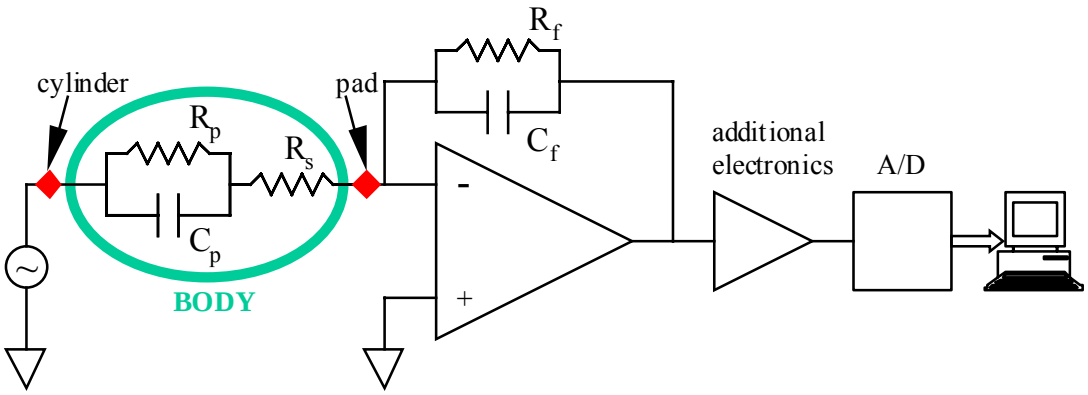

Figure 3.

Dipole Model

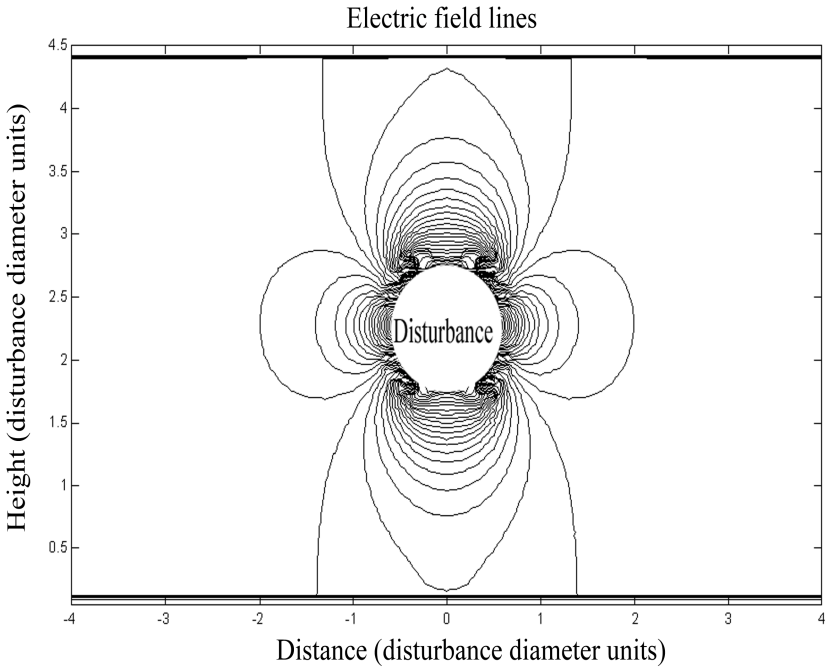

Figure 4.

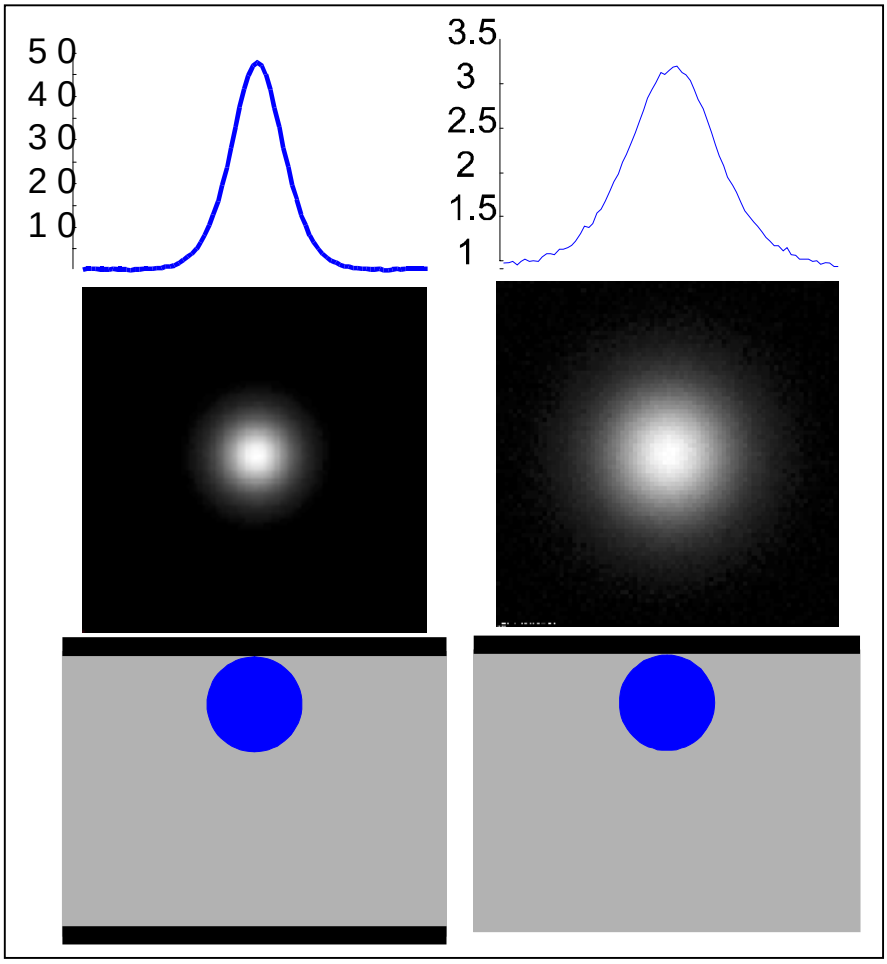

Figure 5.